

Magnetic, transport, and thermoelectric properties of the delafossite oxides $\text{CuCr}_{1-x}\text{Mg}_x\text{O}_2$ ($0 \leq x \leq 0.04$)

T. Okuda, N. Jufuku, S. Hidaka, and N. Terada

Department of Nano-structures and Advanced Materials, Kagoshima University, Kagoshima 890-0065, Japan

(Received 9 March 2005; revised manuscript received 19 July 2005; published 3 October 2005)

We investigated the structural, magnetic, transport, and thermoelectric properties of polycrystalline delafossite oxides, $\text{CuCr}_{1-x}\text{Mg}_x\text{O}_2$ ($0 \leq x \leq 0.04$). We found that, with the substitution of Mg^{2+} ions at the Cr site, the resistivity and Seebeck coefficient drastically decrease without a change of Néel temperature ($T_N=26$ K). In contrast to the x -independent T_N , the deduced Curie-Weiss temperature linearly varies from -170 to -100 K with the increase of x . A crossover occurs in the conductivity from a thermal activation behavior to variable range-hopping one at T_{cross} , around which the temperature dependence of magnetization starts to deviate from the Curie-Weiss form. Furthermore, the negative magnetoresistance effect for $\text{CuCr}_{0.96}\text{Mg}_{0.04}\text{O}_2$ compound is observed only in the variable range-hopping regime and is enhanced around T_N . These results clearly indicate the coupling between the doped hole and the local spin at the Cr site.

DOI: 10.1103/PhysRevB.72.144403

PACS number(s): 75.50.Ee, 72.20.Pa

CuMO_2 (M being a trivalent cation) with delafossite structure has received much attention as a promising candidate for p -type conducting transparent oxides.¹ Charge carriers are introduced into these oxides by the incorporation of excess oxygen or the substitution of the M^{3+} cation for one having a valence less than $3+$. Some thin films of such doped delafossite oxides have a wide band gap above 3.1 eV and a large mobility μ . In these thin films, the carrier density n is kept small so that the *plasma frequency* ($\propto n^{1/2}$) is kept sufficiently low for the materials to become transparent in spite of their large electric conductivity, σ .²

Such delafossite oxides are also one of the possible candidates for a good thermoelectric material. This is because they have a large σ value with low n . Since the Seebeck coefficient usually increases with the decrease of n ,³ they may have a large σ value and large Seebeck coefficient S at the same time; this results in a large thermoelectric figure of merit Z (being defined by $Z=S^2\sigma/\kappa$, where S is the Seebeck coefficient, σ and κ the electric conductivity and the thermal conductivity, respectively.) Another reason is the layered structure of delafossite oxides (Fig. 1). This hexagonal layered structure belongs to space group $R\bar{3}m$ and can be described as the alternate stacking of edge-shared MO_2^- octahedral layers and O^{2-} - Cu^+ - O^{2-} dumbbell-shaped layers perpendicular to the c axis, where the cations form triangular sublattices. Each Cu^+ ion is linearly coordinated by two O^{2-} ions, and the Cu^+ and O^{2-} ions are bonded covalently. From the viewpoint of thermoelectric properties, such a layered structure may have the advantages found in some other layered thermoelectric materials such as Bi_2Te_3 and NaCoO_2 .⁴

In this paper, we have focused on $\text{CuCr}_{1-x}\text{Mg}_x\text{O}_2$ with delafossite structure (Fig. 1). This system has the largest conductivity among delafossite oxides. In the end compound, the CuCrO_2 , Cr^{3+} ion has the electric configuration $3d^3$, while nonmagnetic Cu^+ ion has that of the $3d^{10}$ closed shell. By substituting a Mg^{2+} ion for the Cr^{3+} ion, holes are introduced and the material becomes a good p -type conductor. Upon doping with 5% Mg, the polycrystalline thin film shows a large σ value, 220 Scm^{-1} , and relatively large opti-

cal transmittance.⁵ In this paper, we describe our investigation of the structural, magnetic, transport, and thermoelectric properties of polycrystalline $\text{CuCr}_{1-x}\text{Mg}_x\text{O}_2$ ($0 \leq x \leq 0.04$) compounds that we conducted to understand their intrinsic nature. We also discuss the interplay between these properties and the possibility of applying them to thermoelectricity.

Polycrystalline samples were prepared by using the standard solid-state reaction. We weighted, mixed, and ground well a powder of Cu_2O , Cr_2O_3 , and MgO with purities of 99.99%, and then calcined the mixture in air at 1000°C for 12 h in an alumina crucible. The obtained mixture was ground and calcined 7 times in air at 1200°C for 100 h with an interval grinding procedure. Then, the resulting powder was pressed into a pellet with a size of 4 mm diameter \times 2–10 mm length and sintered in air at 1200°C . To characterize the polycrystalline samples, we conducted powder x-ray diffraction (XRD) measurements. Rietvelt refinement of XRD patterns for the compounds, $0 \leq x \leq 0.02$, indicated that the samples were single phase, with a hexagonal $R\bar{3}m$ structure. For $x=0.03$ and 0.04 compounds, one tiny peak of tetragonal distorted spinel of CuCr_2O_4 appeared around $2\theta = 35.7$ degrees and with x above 0.05, some finite impurity

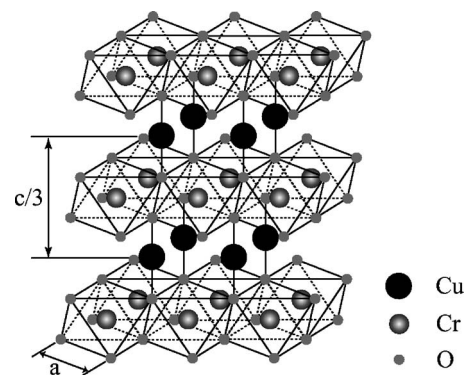


FIG. 1. Delafossite structure where the Cu^+ cation is in twofold linear coordination to O^{2-} and the Cr^{3+} cation is in octahedral coordination.

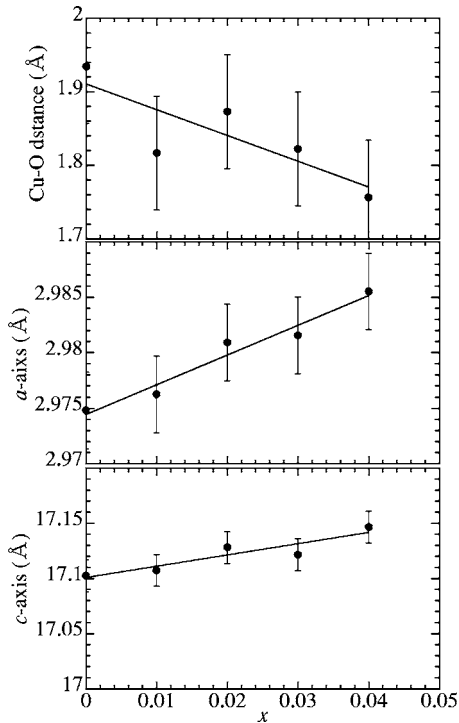


FIG. 2. Variation of the lattice constant a and c of powdered $\text{CuCr}_{1-x}\text{Mg}_x\text{O}_2$ at room temperature as function of Mg content x .

peaks appeared. Thus, in this paper we confine our arguments to the data with x below 0.04. Magnetization measurements were performed with a superconducting quantum interference device magnetometer. Resistivity was measured with the conventional four-probe method, and the Seebeck coefficient was measured with the steady-state method.⁶

The x dependence of lattice parameters at room temperature is shown in Fig. 2. The obtained a - and c -axis lengths of CuCrO_2 are consistent with the previous results⁷ within experimental error. The Cu-Cu distance (a -axis length) is as small as other conductive delafossite oxides such as CuAlO_2 and CuGaO_2 .⁷ This value suggests that the interaction between the closed-shell $\text{Cu}^+(3d^{10})$ ions is not negligible in the electric nature of the Cu layers, and gives the anisotropy of electric conductivity observed in CuAlO_2 laminar crystal⁸ with the smallest Cu-Cu distance (2.86 Å). With the increase of x , both a - and c -axis lengths increased linearly, while the Cu-O distance becomes shorter as the Cu-Cu distance increases. Such a competition between Cu-Cu and Cu-O bonding is generally observed in the CuMO_2 delafossites.⁹ Substituting Mg^{2+} for Cr^{3+} could result in the mixed valence state of either $\text{Cr}^{3+}/\text{Cr}^{4+}$ or $\text{Cu}^+/\text{Cu}^{2+}$. The Cr^{4+} state is normally formed under high oxygen pressure; then, the observed bond length changes associated with the Mg doping seem to support the latter case.

Figure 3 shows the temperature T dependence of magnetization M of $\text{CuCr}_{1-x}\text{Mg}_x\text{O}_2$ ($0 \leq x \leq 0.03$) at 0.5 T. In the figure, all compounds are in the paramagnetic state at 300 K, and the magnetic susceptibility ($\chi = M/H$) obeys a Curie-Weiss form [$\chi = C/(T + \Theta_{CW})$]. The magnetic coupling parameter Θ_{CW} (≥ 0) linearly decreases with the increase of x , as shown in Fig. 4. In the T dependence of M for CuCrO_2 ,

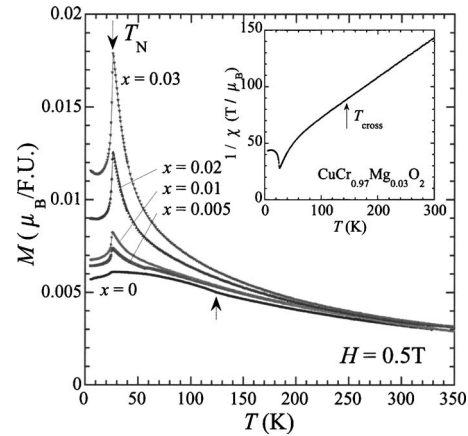


FIG. 3. Temperature dependence of magnetization M for $x=0, 0.005, 0.01, 0.02$, and 0.03 . The inset shows the temperature dependence of inverse susceptibility for $\text{CuCr}_{0.97}\text{Mg}_{0.03}\text{O}_2$.

two anomalies appear at 26 K and around 125 K. The anomaly at the higher temperature disappears with a slight increase of x . On the other hand, we attribute the one at 26 K to an antiferromagnetic (AF) transition. The Néel temperature T_N is almost consistent with the one (25 K) previously reported,¹⁰ but is quite different from the deduced Θ_{CW} values. Furthermore, in contrast to Θ_{CW} , T_N does not change at all within the experimental error with variations of x shown in Fig. 4.

The T dependence of resistivity ρ for each compound is shown in Fig. 5. The values of ρ at 300 K for $x=0, 0.005, 0.01, 0.02$, and 0.03 are 275, 1.5, 0.83, 0.12, and $0.064 \Omega \text{ cm}$, respectively. As shown in the inset of Fig. 5(b), in the T region from 350 K to T_{cross} , all compounds show a

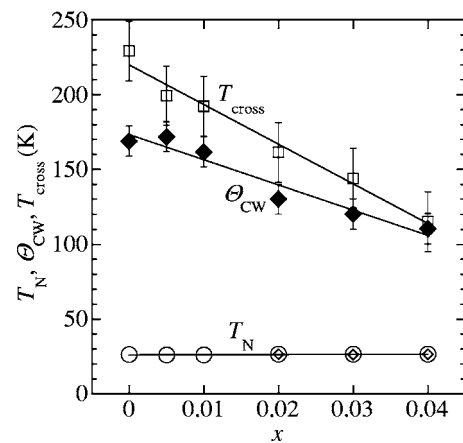


FIG. 4. The x dependence of the Néel temperature T_N deduced from the magnetization data (open circles) and the resistivity (open diamonds), the magnetic coupling parameter Θ_{CW} (solid diamonds), and T_{cross} (open square) at which the electric conductivity deviates from a thermal activation behavior. The straight lines are the guides for the eye.

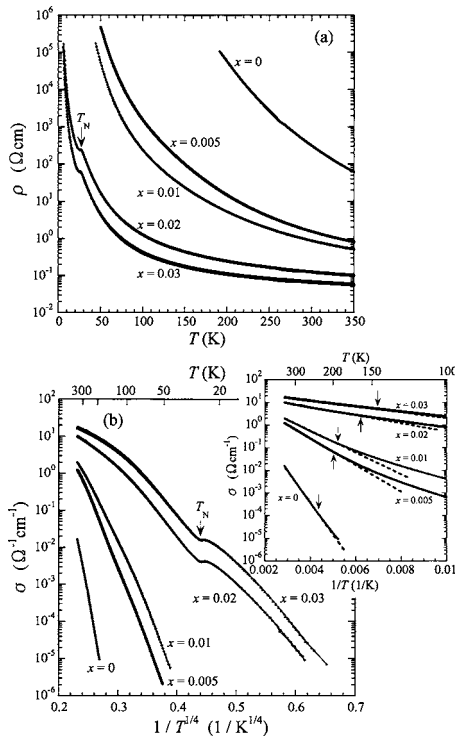


FIG. 5. Temperature dependence of (a) the resistivity ρ and (b) the electric conductivity σ for $x=0, 0.005, 0.01, 0.02,$ and 0.03 . The inset of (b) shows the Arrhenius plot of σ , where the arrows show T_{cross} at which the electric conductivity for each compound starts to deviate from the thermal activation behavior.

thermal activation behavior and σ is well proportional to $\exp(-E_a/k_B T)$, where E_a is the thermal activation energy. The estimated E_a values for $x=0, 0.05, 0.1, 0.2,$ and 0.3 are 278, 119, 95, 36, and 26 meV, respectively. In this temperature region, the hopping of doped holes between the nearest-neighbor Cu sites may determine the electric transport properties. Below T_{cross} , a crossover from thermal activation behavior to that of three-dimensional variable range hopping¹¹ as expressed by $\ln \sigma \propto -(1/T)^{1/4}$ occurs. This crossover was previously observed in CuCrO_2 (Ref. 12) and $\text{CuCr}_{0.95}\text{Mg}_{0.05}\text{O}_2$ thin film.⁵ In this lower temperature region, the decrease of the thermal energy perhaps depresses the hopping between the nearest-neighbor Cu sites, and the contribution of the hopping to the Cr sites become dominant. Hence, the hopping to the Cu site in the other Cu layers becomes relatively dominant so that the conductivity shows the three-dimensional variable range-hopping behavior. As shown in Fig. 5, anomalies appear for $x=0.02$ and 0.03 compounds just at $T_N=26$ K. This suggests that the AF transition can be attributed to AF spin ordering at the Cr site, and the spin- and electric-state of Cr^{3+} ions largely contributed to the electric conductivity. This is manifested by the negative magnetoresistance effect, as discussed later. Below T_N , $\ln \sigma$ also exhibits $(1/T)^{1/4}$ dependence, and the activation energy for variable range hopping below and above T_N seems to be almost the same value.

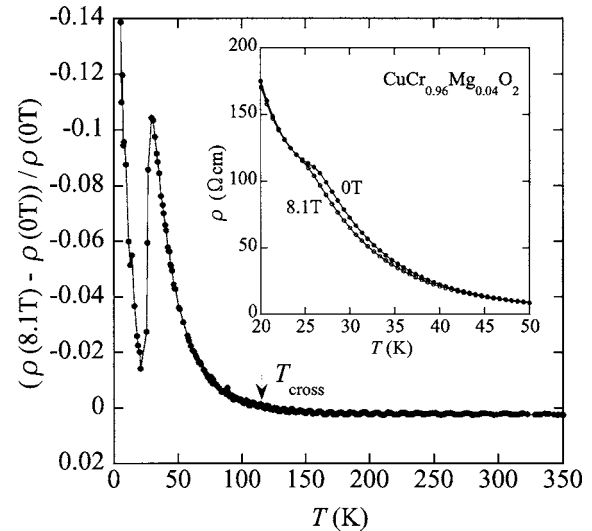


FIG. 6. Temperature dependence of the magnetoresistance $[\rho(8.1 \text{ T}) - \rho(0 \text{ T})] / \rho(0 \text{ T})$ for $x=0.04$ compound. The inset shows the temperature dependence of the resistivity around T_N with and without a magnetic field of 8.1 T.

In addition to the kink structure around the AF transition, a phenomenon occurs revealing the coupling between the magnetic and electric transport properties of these compounds. The crossover in the electric conductivity from the thermal activation behavior to that of variable range hopping occurs at T_{cross} , around which the T dependence of magnetization starts to deviate from the Curie-Weiss form. (T_{cross} for $x=0, 0.005, 0.01, 0.02, 0.03,$ and 0.04 are estimated to be 230 ± 20 K, 199 ± 20 K, $192 \text{ K} \pm 20$ K, 161 ± 20 K, 144 ± 20 K, and 115 ± 20 K, respectively, which show similar values and x dependence to those of Θ_{CW} .) Such spin-charge coupling phenomenon may be explained by the following scenario: The Curie-Weiss-type behavior in the higher temperature region comes from both the local spin ($S=3/2$) at the Cr sites and the Cu^{2+} ions ($S=1/2$) as discussed in other system.¹³ With a further decrease of temperature far below the activation energy, the hole hopping to the Cr site becomes dominant due to the suppression of the hopping between the nearest-neighbor Cu sites. Consequently, the spin fluctuation of the local spin at Cr site is induced at a lower temperature by disturbance due to the hole hopping, so that the susceptibility has an additional component and the behavior deviates from that of Curie-Weiss. If this scenario is correct, one could reasonably imagine that the increase of hole hopping between the nearest-neighbor Cu sites suppressed T_{cross} and the fluctuation of the local spin at Cr site was much further enhanced for the higher x compounds due to the enhancement of disturbance by holes.

This scenario seems to be supported by a magnetoresistance (MR) effect under 8.1 T. Figure 6 shows the T dependence of the magnetoresistance $[\rho(8.1 \text{ T}) - \rho(0 \text{ T})] / \rho(0 \text{ T})$ for $\text{CuCr}_{0.96}\text{Mg}_{0.04}\text{O}_2$. In the variable range-hopping regime, the negative MR is clearly observed, which shows the maximum value ($>10\%$) just above T_N (~ 30 K). After showing the minimum value at about 20 K, it again increases with the decrease of temperature. The enhancement of the MR effect

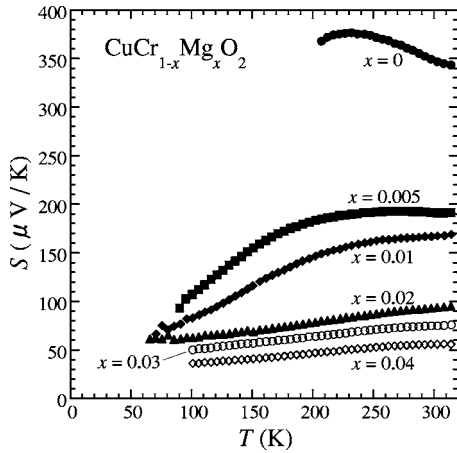


FIG. 7. Temperature dependence of the Seebeck coefficient S for $x=0, 0.005, 0.01, 0.02,$ and 0.03 .

around the magnetic transition temperature is a typical behavior of spin-charge coupling systems such as manganites.¹⁴ It is noted that the negative MR effect appears only in the variable range-hopping regime below around T_{cross} . These results strongly suggest that the hopping holes are correlated with the local spins at the Cr sites in this regime. On the other hand, a tiny positive MR effect was observed in the thermal activation regime above around T_{cross} . The positive MR effect is perhaps one due to the Lorentz force acting on holes. The result in the thermal activation regime does not indicate any correlation between the hole and the local spin at the Cr site, which suggests that the main conduction path is the close-packed Cu layer in this temperature regime.

To discuss the possibility of applying $\text{CuCr}_{1-x}\text{Mg}_x\text{O}_2$ to thermoelectricity, the T dependence of the Seebeck coefficient S is presented in Fig. 7. For all compounds, the positive sign of the Seebeck coefficient indicates p -type characteristics. The S value for $x=0$ is about $350 \mu\text{V}/\text{K}$ at 300 K , and the T dependence shows a broad peak structure. With the increase of x , the S value at 300 K drastically decreases down to about $50 \mu\text{V}/\text{K}$ for $x=0.04$. The broad peak structure in the T dependence gradually disappears with x . The S for x above 0.02 becomes nearly proportional to T below and near 270 K , corresponding to the drastic decrease of the resistivity. Such variation of T dependence with x perhaps originates in the increase of the Fermi degeneracy temperature with the increase of n , as observed in the other transition metal oxides.⁶ Note that there is no clear anomaly around T_{cross} in the T dependence of S . From these transport properties, we can see that the system becomes a more metallic one with the increase of x . The power factors (PF) at 300 K for $x=0, 0.005, 0.01, 0.02,$ and 0.03 are estimated to be $4.4 \times 10^{-4}, 2.5 \times 10^{-2}, 3.4 \times 10^{-2}, 7.3 \times 10^{-2},$ and $8.7 \times 10^{-2} \text{ mW}/\text{K}^2 \text{ cm}$, respectively. The maximum PF is about 25 times smaller than the $\text{CuCr}_{1-x}\text{Mg}_x\text{O}_2$ film⁵ and about 300 times smaller than the best p -type thermoelectric oxides such as NaCoO_2 . Then, the obtained polycrystalline $\text{CuCr}_{1-x}\text{Mg}_x\text{O}_2$ compounds are not suitable for thermoelectricity. This is because the ρ value does not decrease so much with the increase of x and remains a relatively large value of

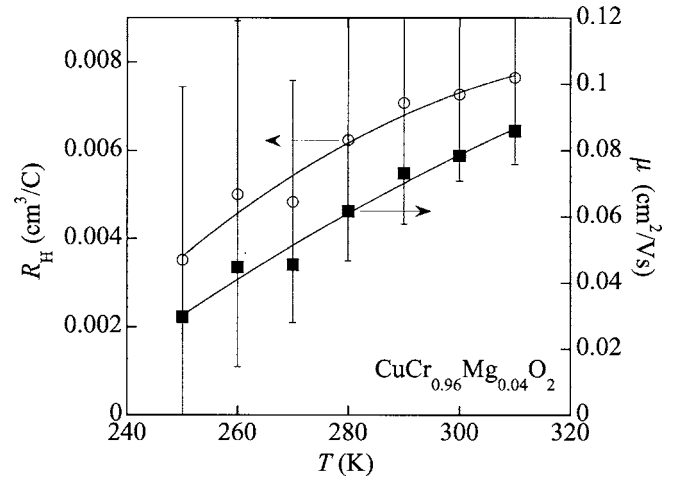


FIG. 8. Temperature dependence of the Hall coefficient R_H and the Hall mobility ($\mu=R_H\sigma$) for $x=0.04$ compound.

$0.064 \Omega \text{ cm}$ for $x=0.03$, while the S value drastically decreases to about $70 \mu\text{V}/\text{K}$ for $x=0.03$. The low packing factor, about 60%–65% for each compound, is one of the reasons for the higher resistivity than that of film. If we could grow a single crystal and use the in-plane conductivity, the PF value would be much improved, because in-plane conductivity should be greater than out-of-plane conductivity, as is the case of the CuAlO_2 laminar crystal.⁸

If we assume that the nominal number of holes are introduced into the compounds, the mobility μ estimated from the relation $\sigma=ne\mu$ are about $0.034, 0.031, 0.11, 0.13,$ and $0.085 \text{ cm}^2/\text{Vs}$ at 300 K for $x=0.005, 0.01, 0.02, 0.03,$ and 0.04 , respectively. According to the Jonker plot (S vs σ), the mobility seems to increase with the increase of x and decrease with the decrease of T . To discuss the μ in detail, we actually measured a Hall coefficient R_H under a magnetic field of 8.1 T . Figure 8 shows the T dependence of R_H for $x=0.04$. We could not measure Hall coefficients for other compounds because of bad signal-to-noise ratios. The observed positive sign of R_H also indicates the p -type characteristics and the hole number estimated from the relation $R_H=1/ne$ is about $8.7 \times 10^{20} \text{ cm}^{-3}$ at 300 K , which is almost consistent with the nominal value. The estimated Hall mobility ($\mu=R_H\sigma$) from the observed R_H is about $0.078 \text{ cm}^2/\text{Vs}$ at 300 K and decreases with the decrease of temperature, which is roughly consistent with those of the above discussion. However, the estimated number increases with the decrease of temperature, which is an unusual behavior. Then, these results indicate that, instead of the simple model on the basis of the Boltzmann transport in a simplified degenerate parabolic band, a more complicated model is needed to discuss the transport properties quantitatively.

In summary, we investigated the structural, magnetic, electric transport, and thermoelectric properties of polycrystalline delafossite oxides $\text{CuCr}_{1-x}\text{Mg}_x\text{O}_2$ ($0 \leq x \leq 0.04$). With the substitution at the Cr site of the Mg^{2+} ion, the compound becomes a p -type conductor around room temperature. This is manifested by a positive sign for Seebeck coefficients S and Hall coefficients R_H and by a drastic decrease of

resistivity ρ . In contrast to the x -independent Néel temperature ($T_N=26$ K), the deduced Curie-Weiss temperature Θ_{CW} linearly decreases from -170 to -100 K with the increase of x . A conductivity crossover seems to occur from thermal activation behavior to one of three-dimensional variable range hopping at T_{cross} , around which the temperature dependence of magnetization starts to deviate from the Curie-Weiss form. Furthermore, the negative magnetoresistance (MR) effect appears only in the variable range-hopping regime under 8.1 T and the MR effects are enhanced around T_N , while the tiny positive MR effect appears in the thermal activation regime.

These features clearly indicate the coupling between the doped hole and the local spin at the Cr site. The former appears dominant at higher temperature and the latter at lower temperature. In order to investigate the intrinsic nature of $\text{CuCr}_{1-x}\text{Mg}_x\text{O}_2$ compounds in detail, further investigation using a single crystal is required.

We would like to thank Z. Hiroi for his help with the Hall and magnetoresistance measurements. This work was supported in part by a research grant from the Iwatani Naoji Foundation, the Nissan Science Foundation, and the Sumitomo Foundation.

-
- ¹H. Kawazoe, M. Yasukawa, H. Hyodo, M. Kurita, H. Yanagi, and H. Hosono, *Nature (London)* **389**, 939 (1997).
²G. Thomas, *Nature (London)* **389**, 907 (1997).
³G. D. Mahan, B. Sales, and J. Sharp, *Phys. Today* **50**(3), 42 (1997); G. D. Mahan, *Solid State Phys.* **51**, 81 (1998).
⁴I. Terasaki, Y. Sasago, and K. Uchinokura, *Phys. Rev. B* **56**, R12685 (1997).
⁵R. Nagarajan, A. D. Draeseke, A. W. Sleight, and J. Tate, *J. Appl. Phys.* **89**, 8022 (2001).
⁶T. Okuda, K. Nakanishi, S. Miyasaka, and Y. Tokura, *Phys. Rev. B* **63**, 113104 (2001).
⁷M. Shimode, M. Sasaki, and M. Kukaida, *J. Solid State Chem.* **151**, 16 (2000).
⁸M. S. Lee, T. Y. Kim, and D. Kim, *Appl. Phys. Lett.* **79**, 2028 (2001).
⁹R. Nagarajan, N. Duan, M. K. Jayaraj, J. Li, K. A. Vanaja, A. Yokochi, A. Draeseke, J. Tate, and A. W. Sleight, *Int. J. Inorg. Mater.* **3**, 265 (2001).
¹⁰R. N. Attili, M. Uhrmacher, K. P. Lieb, L. Ziegeler, M. Mekata, and E. Schwarzmann, *Phys. Rev. B* **53**, 600 (1996).
¹¹N. F. Mott, *Metal-Insulator Transitions* (Taylor & Francis, London, 1990).
¹²S. Mahapatra and S. A. Shivashankar, *Chem. Vap. Deposition* **9**, 238 (2003).
¹³H. S. Kim, B. S. Lee, S. H. Ji, H. Kim, D. Kim, Y. E. Ihm, and W. K. Choo, *Phys. Status Solidi B* **241**, 1545 (2004).
¹⁴M. Imada, A. Fujimori, and Y. Tokura, *Rev. Mod. Phys.* **70**, 1039 (1998).